Journal of Materials Chemistry A

Highly Efficient Photoanode Based on Cascade Structural Semiconductor of Cu2Se/CdSe/TiO2: A Multifaceted Approach to Achieving Microstructural and Compositional Controls

Journal:	*Journal of Materials Chemistry A*
Manuscript ID	TA-ART-11-2015-009179.R1
Article Type:	Paper
Date Submitted by the Author:	n/a
Complete List of Authors:	Zhu, Wen; University of Nottingham, chong, baohe; Huazhong University of Science and Technology, liu, yong; Huazhong University of Science and Technology, Guan, Li; University of Nottingham, Energy and Sustainability Research Division Chen, George; University of Nottingham, Department of Chemical and Environmental Engineering
Note: The following files were submitted by the author for peer review, but cannot be converted to PDF. You must view these files (e.g. movies) online.	
Cover Letter.docx	

SCHOLARONE™
Manuscripts

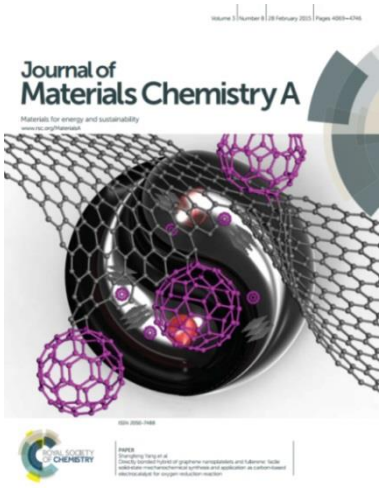

Journal of Materials Chemistry A

Materials for Energy and Sustainability

Full paper submission

Journal of Materials Chemistry A is a weekly journal in the materials field. The journal is interdisciplinary, publishing work of international significance on all aspects of materials chemistry related to energy and sustainability. Articles cover the fabrication, properties and applications of materials.

2014 Partial Impact Factor of *Journal of Materials Chemistry A*: **7.443**
For more information go to www.rsc.org/materialsA

The following paper has been submitted to *Journal of Materials Chemistry A* for consideration as a **Full paper**.

Journal of Materials Chemistry A wishes to publish original research that demonstrates **novelty and advance**, either in the chemistry used to produce materials or in the properties/applications of the materials produced. Work submitted that is outside of these criteria will not usually be considered for publication. The materials should also be related to the theme of materials for energy and sustainability.

Routine or incremental work, however competently researched and reported, should not be recommended for publication if it does not meet our expectations with regard to novelty and impact.

It is the responsibility of authors to provide fully convincing evidence for the homogeneity and identity of all compounds they claim as new. Evidence of both purity and identity is required to establish that the properties and constants reported are those of the compound with the new structure claimed.

Thank you for your effort in reviewing this submission. It is only through the continued service of referees that we can maintain both the high quality of the publication and the rapid response times to authors. We would greatly appreciate if you could review this paper in **two weeks**. Please let us know if that will not be possible.

Once again, we appreciate your time in serving as a reviewer. To acknowledge this, the Royal Society of Chemistry offers a **25% discount** on its books: http://www.rsc.org/Shop/books/discounts.asp. Please also consider submitting your next manuscript to *Journal of Materials Chemistry A*.

Best wishes,

Miss Ruth Norris
Managing Editor, *Journal of Materials Chemistry A*

Dr Fiona McKenzie
Executive Editor, *Journal of Materials Chemistry A*

Journal Name

RSCPublishing

ARTICLE

Highly Efficient Photoanode Based on Cascade Structural Semiconductor of $Cu_2Se/CdSe/TiO_2$: A Multifaceted Approach to Achieving Microstructural and Compositional Controls

Cite this: DOI: 10.1039/xoxxoooooox

Received ooth March 2015,
Accepted ooth May 2015

DOI: 10.1039/xoxxoooooox

www.rsc.org/

Baohe Chong,[abc] Wen Zhu,*[abc] Yong Liu,[a] Li Guan[b] and George Z. Chen*[b]

Hydrogen produced by splitting water is receiving significant attention due to the rising global energy demand and growing climate concern. The photocatalytic decomposition of water converts solar energy into clean hydrogen, and may help mitigate the crisis of fossil fuel depletion. However, the photocatalytic hydrogen production remains challenging to obtain high and stable photoconversion efficiency. Here, we report a highly efficient photoanode based on coaxial heterogeneous cascade structure of $Cu_2Se/CdSe/TiO_2$ synthesized via a simple room-temperature and low-cost electrochemical deposition method. The microstructure and composition of the Cu_2Se top layer are regulated and controlled by doping Cu with various amounts in different zones of the $CdSe/TiO_2$ coaxial heterojunction and then using a simple integral annealing process. Surprisingly, a little effort made to achieve the Cu_2Se top layer utilizing such doped $CdSe/TiO_2$ exhibits a significant enhancement in photocatalytic activity. The maximum stable photocurrent density of the sample with the optimal copper zone and doping concentration has reached up to 28 mA/cm^2, which can be attributed to the success in the uniform dispersion of the three-layer heterogeneous nanojunctions among the anatase nanotube wall from top to bottom. This results in a stepwise structure of band-edge levels in the $Cu_2Se/CdSe/TiO_2$ photoelectrode that is conducive to enhancing effectively the separation of the photogenerated electron-hole pair.

Introduction

The photocatalytic decomposition of water, which uses solar energy to split water and produce cheap hydrogen as a clean energy carrier, is believed to be able to help mitigate the crisis of fossil fuel depletion.[1-5] Since Fujishima and Honda firstly reported in 1972 the use of TiO_2 photoanode for the photocatalytic water splitting,[6] extensive studies have been carried out on TiO_2 based nanomaterials due to their high photocatalytic activity, photochemical stability, nontoxicity and low cost. Various nanostructured TiO_2 materials such as nanorods, nanoparticals, nanotubes and nanowries have been fabricated.[7-16] In comparison with the traditional TiO_2 nanocrystal-based photoelectrodes, vertically oriented TiO_2 nanotube arrays (NTAs) prepared on a Ti foil by electrochemical anodization can offer larger specific surface areas without a concomitant decrease in geometric and structural order.[17, 18] Most importantly, the highly ordered one-dimensional nanostructure provides a unidirectional electrical channel for charge transfer, so that photoinduced electron-hole pairs can be effectively separated.[19, 20] However, TiO_2 is a large band-gap semiconductor (3.2 eV),[21, 22] and its activation is limited only in the UV region, which accounts for only 4-5% of the spectrum of solar energy.[23] To extend the photoresponse into the visible light region, sensitizing TiO_2 NTAs with a narrow band-gap semiconductor is deemed to be a promising strategy.[24-26]

Transition-metal chalcogenides semiconductors such as CdS,[27, 28] Cu_2S,[29] $CuInS_2$,[30] CdSe,[31-34] Cu_2Se,[35-39] Cu_2ZnSnS_4[40] and $Cu_2ZnSnSe_4$[41] as the sensitizer of TiO_2 are of current interest to energy-related research due to their narrow band-gap properties. Among these semiconductors, CdSe has been extensively considered for application in sensitizing TiO_2 NTAs on account of its excellent energy band-gap (1.7eV) and good electron mobility (800 $cm^2/V•s$). Currently, the compound semiconductor heterojunction research of $CdSe/TiO_2$ NTAs focuses mainly on the formation of single-junction nano-materials, which generally use

CdSe nanoparticles or single layer nanofilm as the sensitizer.[42] However, the photocatalytic activity of these composite heterojunctions needs improvement, because such single-junction nano-materials often results in rapid charge-carrier recombination that limits electron harvesting.[31] Recently, the conceptual design of multi-junction photoanodes with a multilayered semiconductor co-sensitization structure has demonstrated greater efficiency than the corresponding single-junction photoanodes.[43, 44] Merging the multilayered narrow-band-gap and the TiO_2 large-band-gap semiconductors can result in the formation of multi-heterostructures and produce a novel photocatalyst with continuously changed band gap, thereby effectively enhancing the photoresponse.

Cu_2Se is a typical p-type semiconductor with highly conducting and semi-transparent features. So far there are several interesting reports on using Cu_2Se as an absorber material in photovoltaic devices.[35-39, 45] A widely varying range of band gap energy for Cu_2Se from indirect band gap of 1.1-1.5 eV to direct band gap of 2.0-2.3 eV have been reported. The ability to tailor the band gap energy is directly related to its capability of microscopic controls in composition and structure. This is helpful to achieve the best energy band match in the formation of multi-junction nano-materials. However, for special highly structured TiO_2 NTAs substrates, it has been proven difficult to use the conventional methods for an accurate control of the microstructure and composition of the multilayered coatings that play a critical role in determining the resultant photocatalytic activity. In the present study, we illustrate the growth of a double-layer structure.

Cu_2Se/CdSe nanofilms were grown on TiO_2 NTA electrodes to form a coaxial heterogeneous cascade structure (Scheme 1) using a simple room-temperature, low-cost electrochemical deposition method. Scheme 1 shows the Cu_2Se/CdSe/TiO_2 coaxial heterogeneous structure and the charge-transfer mechanism in a single coaxial heterogeneous structure. The holes migrate to the sensitizer-electrolyte interface and participate in the oxygen production reaction of water splitting. The electrons are transferred to the core material and travel to the back-contact, where they are conducted through the circuit to the counter electrode to participate in the hydrogen production reaction. Such a structure is designed to help improve the contact area between the sensitizer and the TiO_2 surface, exciting the photoelectrons in the sensitizer and smoothly injecting them into the conduction band of TiO_2 NTAs.[46]

The top layer of Cu_2Se is formed by doping Cu in different zone of CdSe/TiO_2 coaxial heterojunction and then using a simple integral annealing process. The microstructural and compositional characteristics of the materials can be controlled and manipulated by simply changing the doping position and the doping quantity. This relatively inexpensive and simple synthesis technique is suitable for industrial production.

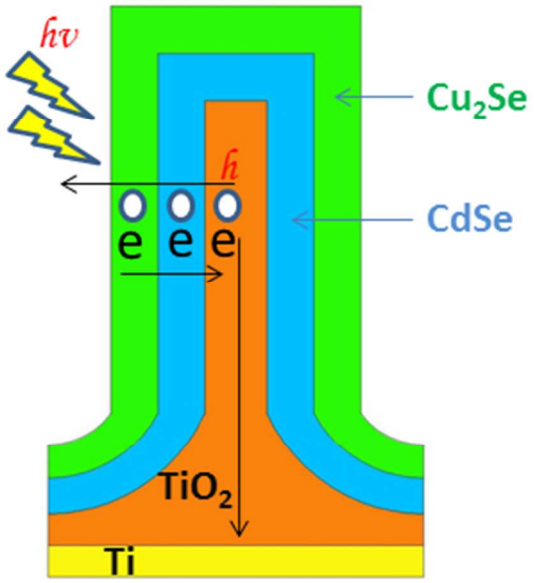

Scheme 1. Cross section of the Cu_2Se/CdSe/TiO_2 coaxial heterogeneous cascade structure with two-junction and the charge-transfer mechanism.

Experimental

Preparation of TiO_2 NTAs.

Synthesis of highly ordered TiO_2 NTAs followed the typical two-step anodic oxidation method.[44] Titanium foils (99.8% purity) were mechanically ground using emery papers with different types and polished with the metallographic abrasive paper successively, then ultrasonically cleaned orderly with acetone, distilled water and ethanol, followed by drying in ambient air (at laboratory temperature

 This journal is © The Royal Society of Chemistry 2015

and common ambient pressure). The anodization of titanium foil was carried out in an electrolyte comprised of NH_4F (0.32 wt. %) and distilled H_2O (2.0 vol %) in ethylene glycol at room temperature using platinum foil as the counter electrode. The two-step anodic oxidation was conducted as follow: step-1, the titanium foil was firstly anodized at 60 V for 20 min. in the electrolyte, followed by rinsing with ethanol and drying in ambient air, and then by annealing at 700 ℃ in a muffle furnace for 1 h with heating rate of 7 ℃/min; step-2, the sample was re-soaked into the electrolyte and suffered the second anodization for 11 h, then was annealed again at 450℃ in the muffle furnace for 2 h at a heating rate of 2℃/min after rinsing with ethanol and drying in an oven at 100℃ for 1 h.

Fabrication of CdSe/TiO_2 and Cu_2Se/CdSe/TiO_2 Coaxial Heterogeneous Nanojunction.

For electrochemical deposition of CdSe on TiO_2 NTAs, $CdSO_4$ and SeO_2 of the analytical reagent grade were used as the sources of Cd and Se, respectively. EDTA-2Na ($C_{10}H_{14}O_8N_2Na_2 \cdot 2H_2O$) and NH_4OH were used to complex the ions and adjust the pH value for obtaining a proper electrodeposition potential. The solutions were freshly prepared just before the beginning of each series of measurements. The electrochemical deposition was carried out using a computer controlled electrochemical workstation that was connected to a three-electrode system comprised of Ti foil as work electrode (WE), Pt foil as counter electrode (CE) and Hg_2Cl_2/KCl (SCE) as reference electrode (RE). For copper doping, $CuSO_4$ (2 mM) solution was used as Cu source.

Characterizations.

The morphologies of the samples were studied by field emission scanning electron microscopy (FESEM) (Nova NanoSEM 450) and transmission electron microscopy (TEM) (JEOL JEM-2100). The X-ray diffraction (XRD) (X'Pert PRO) measurement was performed on a Bruker D8 diffractometer with Cu Ka radiation operated at 40 kV, 40 mA. UV-Vis absorption spectra were collected at room temperature using the Lambda 35 UV-vis spectrophotometer. For the incident-photon-to-current-conversion efficiency (IPCE) measurement, light source was generated by a 300W xenon lamp of Newport(Oriel,69911) and then split into specific wavelength using Newport oriel cornerstone 130 1/8 Monochromator (Oriel,model 74004).
The optical response performance of the samples was investigated in a photoelectrochemical cell with a platinum foil counter electrode and the SCE reference electrode. 0.5 M Na_2S was used as the electrolyte in photoelectrochemical measurements. The CorrtestTM CS350 electrochemical workstation was also used to control the potential and record the photocurrent generated. Xe lamp (CHF-XM35-500W) coupled to an AM 1.5G filter was used as the standard light source throughout the tests. The illumination intensity of 100mW/cm^2 was calibrated with a readout meter for solar simulator irradiance before the measurement. The sample size was 1.0 cm×2.0 cm.

Results and discussion

This research focuses on synthesis of multi-junction nano-materials coated with highly ordered structure through a modified electrochemical atomic layer deposition (ALD) route, and on studying and manipulating their microstructural and compositional properties. The electrochemical ALD method as reported in the literature is based on underpotential deposition (UPD).[47-51] UPD is a surface-limited phenomenon in which the deposition of one element occurs at a potential that precedes the Nerstian equilibrium value, so that the resulting deposit is generally limited to one atomic layer. Electrochemical ALD utilizes alternating UPD of the elements that form the compound semiconductor in a cycle. Each deposition cycle can form only a monolayer of heterogenous elements, and the thickness of the deposit is controlled by the number of deposition cycles. To date, this method has been extensively used to grow highly crystalline nanofilms of transition-metal chalcogenides at ambient temperature and pressure and is convenient for industrial production. Before electrochemical ALD, it is pivotal to find the suitable UPD potential of each compositional element of the compound. This can be determined by cyclic voltammetry (CV). The electrochemistry behaviour of Se(IV) was investigated in an ammonia buffer medium.[49,52] In this regime, two competitive processes were observed: the first led to the formation of Se(0), and the second resulted in further reduction of Se(0) to HSe^-. Thus, it is important to understand which process dominates in the competition, and which exerts a direct impact on the Se UPD behaviour. Apparently, the competition can be affected by a number of factors, such as the type of electrolyte and buffers, pH, complexing agent, temperature, and so on. Therefore, in this study, the addition of EDTA as a complexing agent, the content variation of the ammonia buffer, and a resultant suitable pH value are used to adjust the UPD potential of Se and Cd for the deposition of the CdSe layer. Figure 1 shows the cyclic voltammograms (CVs) of the TiO_2 NTA electrode in the solution of mixed $CdSO_4$ and SeO_2 in the presence of the ammonia buffer and the EDTA complexing agent. It can be seen that both CVs exhibit a reduction peak around -0.6 V, which is indication of the UPD potentials of both Se and Cd being adjusted to a common region. Then, a modified electrochemical ALD was employed to simplify its operating procedures.[53,54] In the modified electrochemical ALD, a constant potential within the common UPD region was chosen and held constant for co-deposition of both elements.[46] In this case, a potential of -0.7V was applied to co-deposit the CdSe nanofilm onto the TiO_2 NT substrate under the UPD condition.

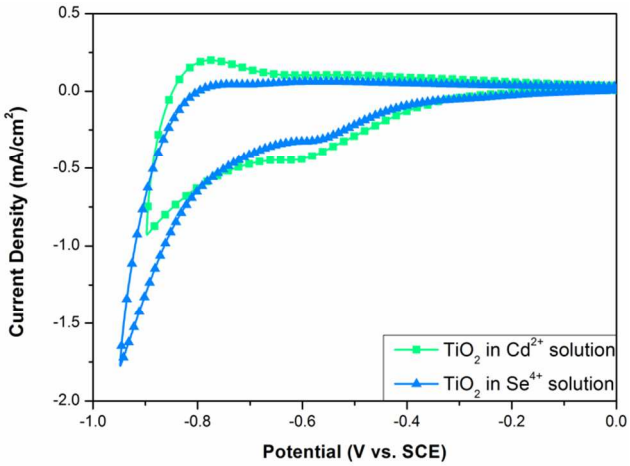

Figure 1. Cyclic voltammograms of the TiO_2 nanotube electrode recorded at 10 mV/s in the solution containing (green line) 10 mM $CdSO_4$ + 0.1M EDTA, PH = 8.5; or (blue line) 2 mM SeO_2 + 0.1M EDTA, PH = 8.5.

Figure 2a shows XRD patterns of the pure TiO_2 NTAs and the as-prepared CdSe/TiO_2 NTAs samples. All diffraction peaks on the black line can be well-indexed to the anatase TiO_2 phase and the Ti metal phase. After decoration of the TiO_2 NTAs with CdSe, the intensity of diffraction peaks of the TiO_2 phase decreased, indicating that the CdSe had been attached onto the TiO_2 NTAs. Meanwhile, some new diffraction peaks located at 24.13°, 42.34°, 49.93° appeared (see red line in Figure 2a). These new peaks were correspondingly attributed to (100), (110), (112) of the hexagonal CdSe (JCPDS No. 03-065-3415), confirming that the deposited CdSe layer possessed the hexagonal crystal structure. Figure 2b shows the EDX quantitative analysis of the CdSe coated or sensitized TiO_2 NTAs. Both Ti and O peaks came from the TiO_2 NTAs, while Cd and Se peaks that were clearly visible on the EDX spectrum came from the CdSe deposit. Quantitative analysis of the EDX spectrum revealed that the atomic ratio of Cd (2.39%) versus Se (2.53%) was nearly 1, indicating that the deposited CdSe had the expected 1:1 stoichiometry.

a

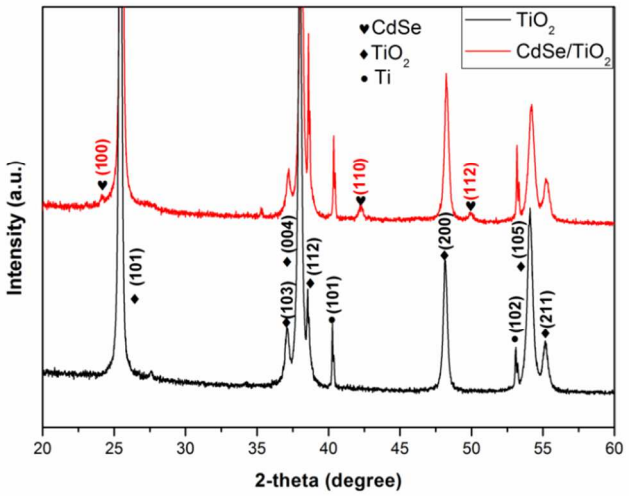

This journal is © The Royal Society of Chemistry 2015

b

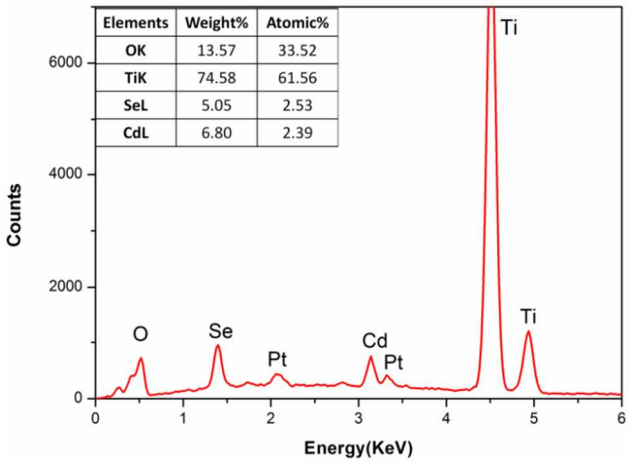

Figure 2. (a) XRD diffractograms of samples: (black line) pure TiO_2; (red line) CdSe(7h)/TiO_2. (b) EDX spectrum and the corresponding element content of CdSe(7h)/TiO_2

The photocurrent-potential curves measured on a series of CdSe/TiO_2 NTAs samples are shown in Figure 3. The CdSe layers in these samples were fabricated using five different deposition times; data for the corresponding pure TiO_2 NTAs substrate before sensitization is also provided. The stable photocurrent density of pure TiO_2 NTAs was about 2.0mA/cm^2 (the current density is measured against the projected area of the TiO_2 NTAs). After deposition of CdSe on the TiO_2 NTAs using the electrochemical ALD method, the improvement of photocurrent densities of CdSe/TiO_2 NTAs were obvious. Especially, a noteworthy enhancement in the photocurrent density was found for the CdSe(7h)/TiO_2 sample in which the CdSe layer was deposited for 7 h. As shown in Figure 3, the photocurrent density increases in the wake of the increasing CdSe deposition time within 7 h. However, when the deposition time was further increased to 9 h, the photocurrent density dropped, indicating that the sensitized CdSe layer was too thick after 9 h of deposition. Excessive CdSe deposition causes reduced light absorption because of the increase of the transmission distance of photons.

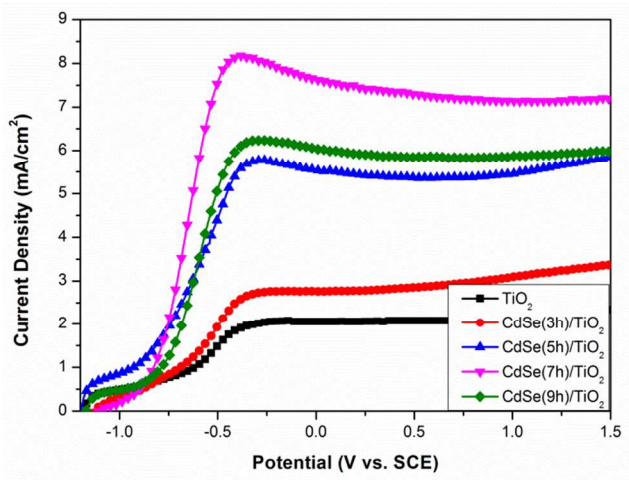

Figure 3. Optical response of CdSe/TiO_2NTAs samples in which the CdSe layers are fabricated using different deposition times compared with pure TiO_2.

The CdSe(7h)/TiO_2 electrode was then selected as the optimal seed layers on account of its best photocurrent density in this work. Before doping Cu into the CdSe nanofilm, a suitable potential for Cu deposition on the CdSe underlayer should be determined. Figure 4 features the CV of CdSe substrate in the Cu ion solution. For comparison, the CV of CdSe in the blank solution (without Cu ion) is also provided in Figure 4 (green line). A relatively broad anodic stripping peak A1 was observed between -0.55 and -0.3 V. This strip peak means the decomposition of CdSe from the TiO_2 substrate if an applied potential is more positive than -0.55 V. The blue line shows the first CV cycle of CdSe/TiO_2 in the Cu^{2+} solution, in which the region C between -0.6 to -0.35 V indicates the UPD region of Cu on the CdSe substrate. When the scan region extends negatively to -1.0 V, two anodic peaks A2 at -0.3 V and A3 at 0.2 V correspond to the oxidative stripping of Cu deposited at the Nernst potential and via UPD, respectively (pink line). To avoid decomposition of the CdSe substrate during the Cu deposition process, the deposition potential of -0.6 V was selected.

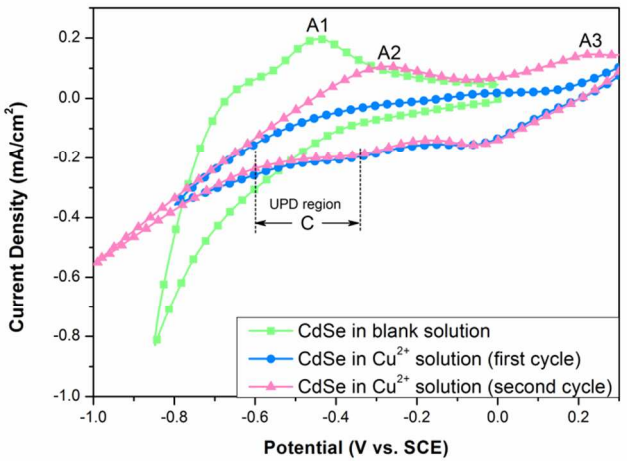

Figure 4. Cyclic voltammogram of CdSe(7h)/TiO_2 nanotube electrode recorded at 10 mV/s in solutions containing (green line) 0.5M Na_2SO_4; (blue and pink line) 2mM $CuSO_4$

Figure 5a shows the XRD patterns of a sample with a structural formula of CdSe(1h)/Cu(0.6C)/CdSe(6h)/TiO_2. This Cu-doped sample was prepared according to the following procedure. Firstly, CdSe was deposited on the TiO_2 NTAs substrate for 6 h using the electrochemical ALD method. Then, copper was deposited on the CdSe(6h)/TiO_2 substrate upon consumption of a charge of 0.6 C. After drying slightly, the Cu covered sample was re-immersed into the CdSe reaction solution and subjected to electrochemical ALD for 1 h. Before testing, the sample was integrally annealed at 450 ^oC in nitrogen (ambient pressure) for 2 h with heating and cooling rate of 2 ^oC/min. As shown in Fig. 5a, in comparison with the XRD pattern of CdSe(7h)/TiO_2 shown in Figure 2, the Cu-doped sample gave new peaks, located at 26.79° and 44.45°, that were attributed to (111) and (220) of Cu_2Se, respectively. Energy dispersive X-ray spectroscopy (EDS) analysis confirmed the presence of Cd, Cu and Se elements in the Cu-doped sample (Figure 5b). Subtracting the amount of Cd that is the same as the amount of Se in the CdSe compound, the atomic ratio of Cu to the remaining Se was very close to 2:1, in consistence with the stoichiometry of Cu_2Se, indicating the effectiveness of the integral annealing process for the formation of the Cu_2Se compound.

a

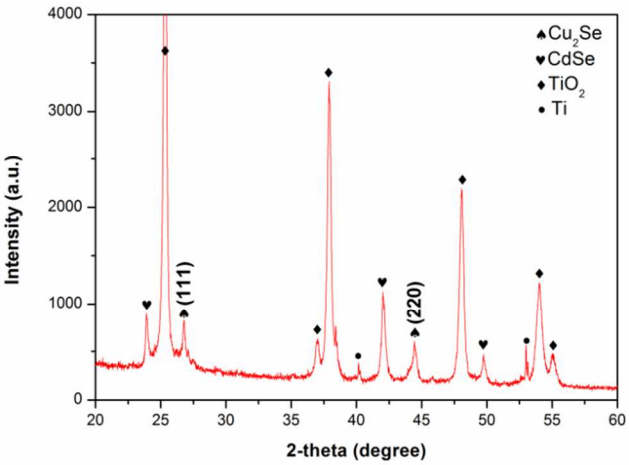

This journal is © The Royal Society of Chemistry 2015

b

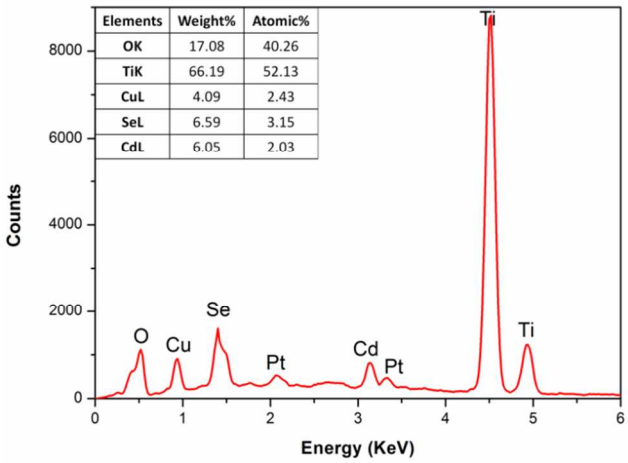

Figure 5. (a) XRD diffractograms of sample CdSe(1h)/Cu(0.6C)/CdSe(6h)/TiO_2; (b) EDX spectrum and the corresponding element content of sample CdSe(1h)/Cu(0.6C)/CdSe(6h)/TiO_2

The FE-SEM images of as-prepared samples including the pure TiO_2 NTAs, CdSe/TiO_2 NTAs and Cu-doped CdSe/TiO_2 NTAs also are shown in Figure S1. The pure TiO_2 NTAs sample presented a highly uniform array of nanotubes of 100 nm in diameter and about 8 nm in wall thickness. These nanotubes were oriented in the vertical direction to the titanium foil substrate. The hollow nature makes both inner and outer surface areas accessible for modification with a narrow band-gap semiconductor. FE-SEM images of the CdSe sensitized TiO_2 NTAs sample revealed that well modified coaxial structures have been obtained successfully using the electrochemical ALD method (Figure S1c,d). The tube inner diameter was shrunken and the wall was thickened relative to those in Figure S1a,b. After CdSe electrodeposition, the average inner diameter of the tubes was ~80 nm, suggesting that the CdSe coating layer was ~10 nm thick (the pure TiO_2 NT substrate had an average inner diameter of 100 nm). Figure S1(e, f) present the FE-SEM images of Cu-doped CdSe/TiO_2 NTAs sample. The tube inner diameter and wall thickness were not significantly different from those of the only CdSe sentitized sample. Because there was an addition of a certain amount of copper, the constant wall thickness suggested that copper has diffused into adjacent CdSe layer, resulting in the formation Cu_2Se during the integral annealing process. Figure S2 shows the corss-sectional FE-SEM images of as-prepared samples including the pure TiO_2 NTAs, CdSe/TiO_2 NTAs and Cu-doped CdSe/TiO_2 TNAs. Cross-sectional FE-SEM image (Figure S2a) reveals that the pure TiO_2 TNAs have a rather smooth wall surface. As shown in Figure S2(b,c) when semiconductor was deposited on the TiO_2 TNAs using the electrochemical ALD method, both the interior and exterior surfaces of TiO_2 NTAs were homogeneously coated with sensitizer without any obvious particle agglomerations, suggesting the electrochemical ALD method in our work is rather efficient to grow well dispersed nanofilms among the whole nanotube wall.

The prepared samples were further investigated using transmission electron microscopy (TEM). Figure 6a features a single tube wall of the pure TiO_2 nanotube sample that shows a hollow nanostructure and has a wall thickness of about 8 nm. The wall is smooth without any stuff covered. Figure 6b and 6c show the TEM images of samples after semiconductor sensitized, which reveal that the semiconductor were uniformly grown on the TiO_2 nanotube inner and outer of wall. The high resolution TEM images (HRTEM) shown in Figure 6d-6f reveal a well-defined cascade structure with uniformly dispersed two and three-layer heterogeneous nanojunction among the anatase nanotube wall has been obtained. In Figure 6f, the d spacing in the outer nanocrystal layer was measured to be 0.32 nm, which matched well the interplanar spacing of Cu_2Se (111) plane and was consistent with the XRD measurement result shown in Figure 5. The d spacing in the interlayer was 0.37 nm and was assignable to the interplanar spacing of the CdSe (100) plane, while the d spacing of 0.35 nm in the inner layer was identifiable to the interplannar spacing of the TiO_2 (101) plane. This result demonstrates that the double-layer Cu_2Se and CdSe co-sensitized TiO_2 NT electrodes with a coaxial heterogeneous cascade structure of Cu_2Se/CdSe/TiO_2 can be successfully formed by doping Cu in CdSe/TiO_2 NTAs followed by the simple integral annealing process.

Journal Name RSCPublishing

ARTICLE

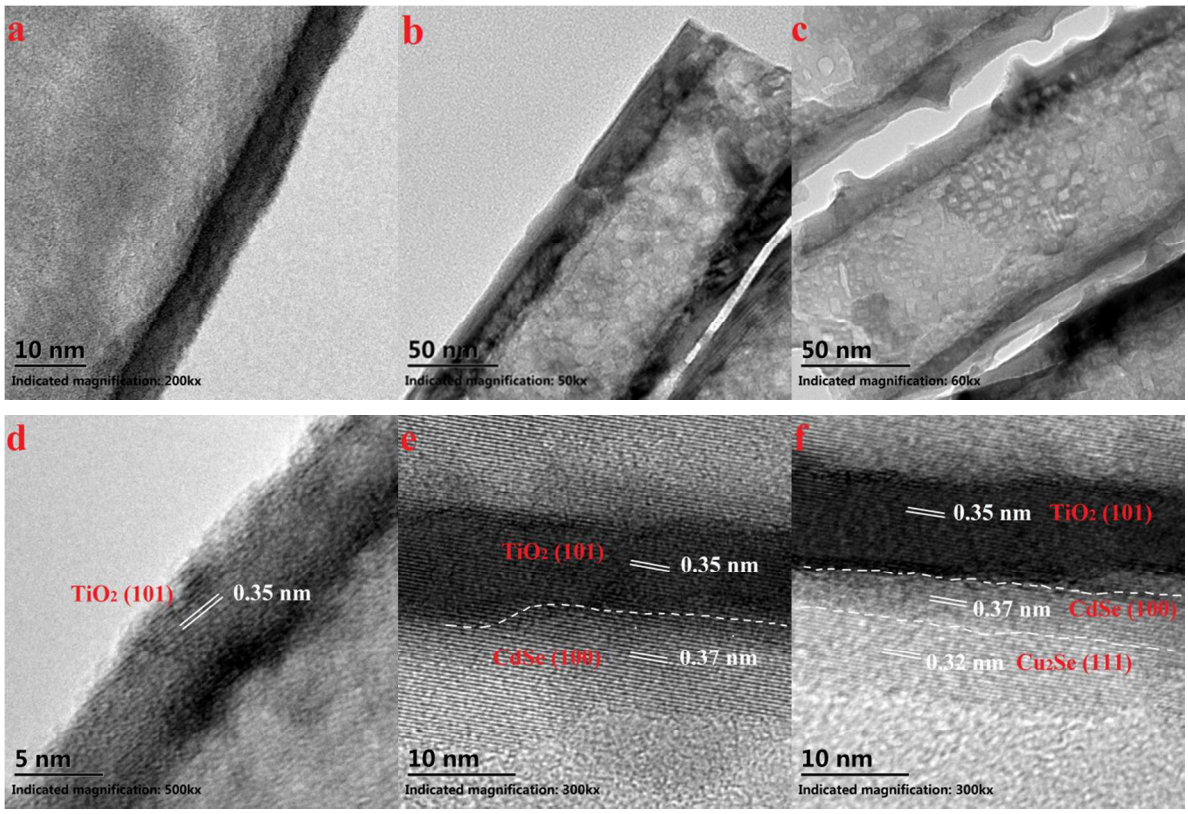

Figure 6 TEM (a,b,c) and HRTEM (d,e,f) image of samples. (a,d) pure TiO2, (b,e) CdSe(7h)/TiO2, (c,f) CdSe(1h)/Cu(0.6C)/CdSe(6h)/TiO2

To investigate an appropriate copper doping zone, Cu was loaded in different deposition period of CdSe. Three different sites were chosen to deposit Cu, including near the inner layer, the intermediate layer and near the outer layer, with corresponding structural formula of CdSe(6h)/Cu(0.3C)/CdSe(1h)/TiO_2, CdSe(3.5h)/Cu(0.3C)/CdSe(3.5h)/TiO_2 and CdSe(1h)/Cu(0.3C)CdSe(6h)/TiO_2, respectively. The amount of charge for deposition of Cu was 0.3 C, while the total deposition time of CdSe was 7 h. Figure 7 shows the measured photocurrent density of three Cu-doped samples with different copper doping sites. The sample of CdSe(1h)/Cu(0.3C)CdSe(6h)/TiO_2 achieved the maximum stable photocurrent density of 20 mA/cm^2 among the samples investigated. In contrast, the sample of CdSe(6h)/Cu(0.3C)/CdSe(1h)/TiO_2 showed only a photocurrent density of 7 mA/cm^2 that was even less than the 7.5 mA/cm^2 level obtained from undoped CdSe(7h)/TiO_2 (see Figure 3). It is generally believed that the charge transfer rate is governed by the energy band alignment at the heterointerfaces.[55-58] Fermi-level alignment between TiO_2, CdSe and Cu_2Se was proposed to construct a stepwise structure of band-edge levels in the Cu_2Se/CdSe/TiO_2 photoelectrode (Scheme 2). Such stepwise energy band structure is advantageous to the electron injection and hole recovery in the system. When the copper doping site is chosen near the outer layer, it gives rise to the formation of Cu_2Se at the top level during the integral annealing process. As a result, a suitable architecture of Cu_2Se/CdSe/TiO_2 can be obtained, which is favourable for reducing the charge-carrier recombination probability. On the contrary, doping copper near the inner layer produces an architecture of CdSe/Cu_2Se/TiO_2 that does not conform to this stepwise band edge level alignment and as a result hinders the photogenerated charge-carrier transfer. A similar effect has been found in the CdSe and CdS co-sensitized TiO_2 semiconductor photoelectrodes in which the photocurrent density of the CdSe/CdS/TiO_2 electrode is higher than that of the CdS/CdSe/TiO_2 electrode.[55, 56, 58] By means of the time-resolved photoluminescence technique, the impact of energy band structure on the charge-carrier transfer has been fully explained.[56]

This journal is © The Royal Society of Chemistry 2015

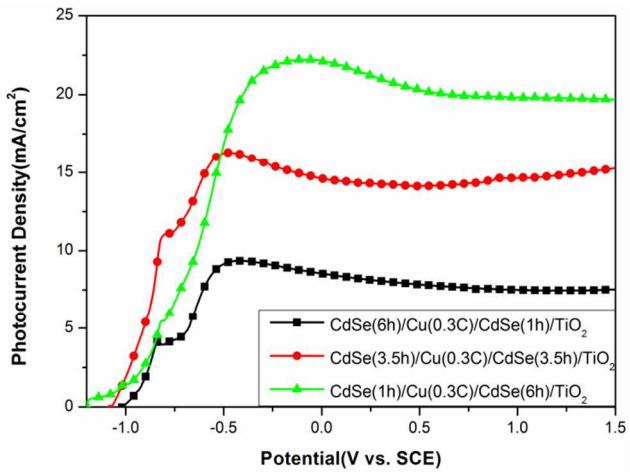

Figure 7. Optical response of Cu-doped CdSe(7h)/TiO_2 with various copper doping zone. The Cu deposition coulomb was 0.3 C, while the total deposition time of CdSe was 7 h.

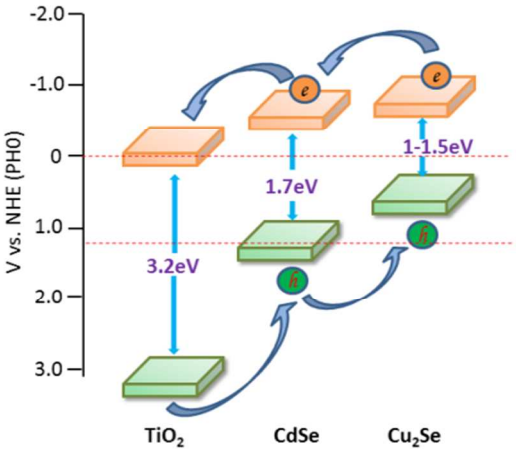

Scheme 2. Ideal step band edge structure for efficient transports of photogenerated charge-carriers in $Cu_2Se/CdSe/TiO_2$ electrode.

Furthermore, the effect of copper doping concentration was studied by adjusting the amount of Cu deposition charge. The variation of photocurrent density as a function of the amount of copper doping in $CdSe/TiO_2$ is shown in Figure 8. The stable photocurrent densities of four samples with various copper doping concentrations of Cu (0.3 C), Cu (0.6 C), Cu (1.2 C), and Cu (1.8 C) were 20, 28, 17 and 13 mA/cm^2, respectively. The maximum photocurrent density can be obtained from the 0.6 C sample. In comparison with TiO_2 NTA, the CdSe(1h)/Cu(0.6C)CdSe(6h)/TiO_2 electrode showed a 14-fold enhancement in photocurrent density.

Practical photoelectrolysis system consists of two electrolyte immersed electrodes with the bias voltage applied between the working and counter electrodes, the overall chemical reaction in such a system is made of two independent half reactions.[56] To understand the chemical changes at the photoelectrode, in laboratorial water photoelectrolysis experiments a three-electrode geometry is used to measure photocurrent. This geometry involves a working electrode (photocathode or photoanode), a counter electrode that generally is platinum and a reference electrode that is SCE electrode in our work. To investigate the difference of photoconversion efficiency between the two-electrode and three-electrode configuration, the photochemical measurement was carried out. Figure S3 shows the measurement results of $CdSe/TiO_2$ and $Cu_2Se/CdSe/TiO_2$ in different configuration. The photocurrent density curves of both $CdSe/TiO_2$ and $Cu_2Se/CdSe/TiO_2$ (Figure S3 a,~~e~~b) shift to positive about 1.2V in the two-electrode configuration with respect to the three-electrode configuration, which attributes to the reference electrode SCE. ~~The photoconversion efficiencies (Figure S3 b,d) calculated according to the corresponding equation shows that the photoconversion efficiency measured in three-electrode configuration have a slight exaggeration (no significant) with respect to the photoconversion efficiency value measured in two-electrode configuration. This result agrees with the literature published pervious.[56] Grimes~~

~~explained that the voltage measured between the working and the counter electrodes gives the actual applied bias voltage V_{app}. This voltage multiplied by the cell current gives the electrical energy supplied by the electrical power supply. But in practice, where a potentiostat is used to apply an external bias to the photoelectrode, this actual voltage V_{app} (between the working and counter electrodes) may slightly exceed the bias voltage measured as $V_{app} = V_{meas} - V_{aoc}$ with respect to the reference electrode. Thus the measurement tested in three-electrode configuration can show a slightly higher efficiency value than that tested in two-electrode configuration.[59]~~

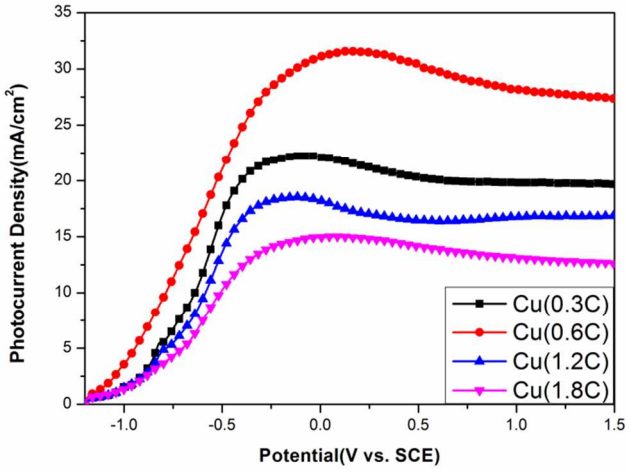

Figure 8. Optical response of different Cu deposition coulomb in CdSe(1h)/Cu/CdSe(6h)/TiO_2 sample.

To quantify the photoresponse of prepared samples, incident-photon-to-current-conversion efficiency (IPCE) measurements were made to examine their photoresponses as a function of incident light wavelength. As revealed in Figure 9a, the CdSe/TiO_2 NTAs showed a pronounced response in the visible light region, with a maximum IPCE value of 31.9% obtained around 500 nm. The photoresponses of CdSe/TiO_2 NTAs were drastically extended to the all visible light region of the solar spectrum after doping Cu into CdSe/TiO_2 NTAs, indicating that semiconductor Cu_2Se can efficiently promote the photoresponse owe to its narrow bad-gap. Overall, the IPCE of CdSe/TiO_2 NTAs and Cu_2Se/CdSe/TiO_2 NTAs revealed significant photoresponses in the visible light region, which is consistent with their corresponding UV-Vis absorption spectra. Figure 9b shows the UV−Vis absorption curves of the pure TiO_2 NTAs, the CdSe/TiO_2 NTAs and the Cu_2Se/CdSe/TiO_2 NTAs. The pure TiO_2 NTAs had an absorption onset at about 400 nm that was determined by linear extrapolation from the inflection point of the curve toward the baseline. The calculated band-gap is 3.1 eV, corresponding to the typical band-gap value of TiO_2. It can be seen that CdSe deposition atop TiO_2 NTAs has a red-shifted absorption edge into the visible region, extending the absorption tail to 650 nm with a band-gap about 1.9 eV. After Cu doping and annealing, the absorption was further red-shifted and has an absorption tail to 800 nm, gaining a band-gap value of 1.5 eV. In addition, the absorbance of the cascade structural Cu_2Se/CdSe/TiO_2 NTAs film is apparently stronger than that of the CdSe/TiO_2 film in the visible region from 400 to 800 nm. The enhanced absorption is believed to result from the formation of the Cu_2Se top layer, which has a narrower band-gap to harvest solar energy in almost the entire visible light zone.

 This journal is © The Royal Society of Chemistry 2015

Journal Name RSCPublishing

ARTICLE

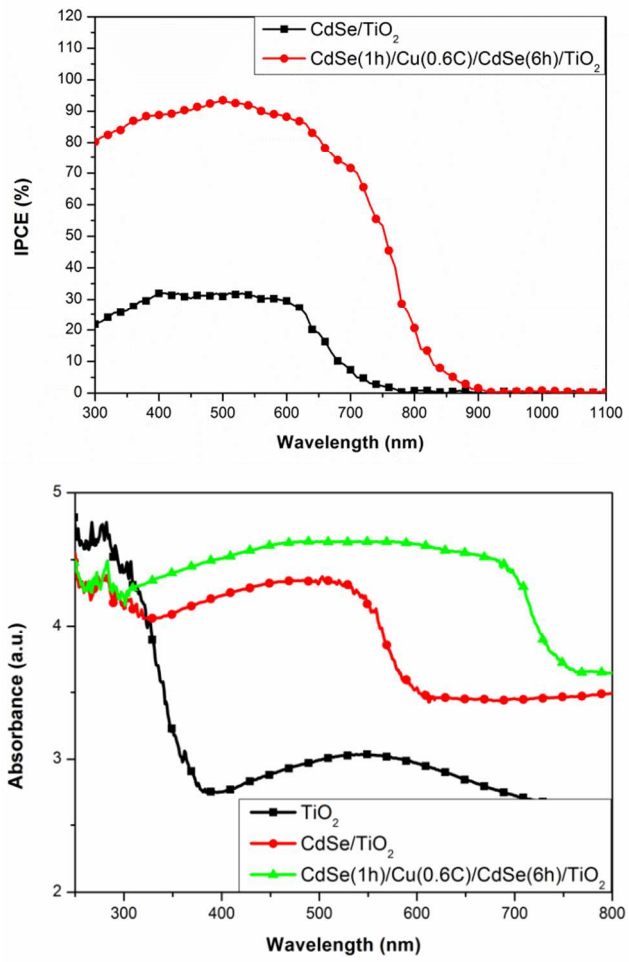

Figure 9. (a) TEM image of sample CdSe(1h)/Cu(0.6C)/CdSe(6h)/TiO_2. (b) UV-vis absorbance spectra of pure TiO2(black line); CdSe(7h)/TiO_2 (red line); CdSe(1h)/Cu(0.6C)/CdSe(6h)/TiO_2 (green line).

Conclusions

In this paper, we have proposed and demonstrated a new method for the fabrication of a novel semiconductor photoanode with a unique Cu_2Se/CdSe/TiO_2 nanostructure. The fabrication is developed on the TiO_2 NTAs substrate in three steps. Firstly, the CdSe inner layer was successfully deposited on pure TiO_2 nanotubes substrate to form a nanotube-array coaxial heterogeneous structure by electrochemical ALD. It was found that CdSe deposition for 7 h had led to a significant improvement in the photocurrent density, reaching 7.5 mA/cm^2. Secondly, the CdSe(7h)/TiO_2 nanotubes were selected as the optimal seed layer for Cu doping. Finally, integral annealing was applied, and the sample with the structural formula of CdSe(1h)/Cu(0.6C)CdSe(6h)/TiO_2 showed the best photoelectrochemical performance.

The product possessed a cascade of multiple heterogeneous junctions formed in the coaxial manner on the TiO_2 NTAs substrate. An accurate control and manipulation in microstructure and composition of the materials could be achieved by simply changing the

doping position and concentration, which is helpful to achieve a best energy band match for splitting water utilizing solar energy. The as-prepared photoanode combines the multifaceted advantages, including the directed vertical electric transport of TiO_2 nanotubes, the good contacts between Cu_2Se and CdSe films, and the significantly enhanced light-harvesting and carrier transporting ability arising from the stepwise band edge level alignment in the resultant cascade structural semiconductor. In comparison with the pure TiO_2 NTAs, the as-prepared Cu_2Se/CdSe/TiO_2 NTAs photoanode showed a 14-fold enhancement in photocurrent density. It is actually encouraging and opens up an avenue for the development of water splitting materials.

Acknowledgements

This work was financed by the Marie Curie IIF Fellowship (623733), the National Natural Science Foundation of China (21173090), the Special Found for Strategic Emerging Industry Development of Shenzhen (JCYJ20120618100557119), and Program for Changjiang Scholars and Innovative Research Team in University (IRT1014). Technical assistance from the Analytical and Testing Center of HUST is gratefully acknowledged.

Notes and references

[a] State Key Laboratory of Materials Processing and Die & Mould Technology, Huazhong University of Science & Technology, Wuhan 430074, People's Republic of China
[b] Department of Chemical and Environmental Engineering, The University of Nottingham, Nottingham NG7 2RD, United Kingdom
[c] Research Institute of Huazhong University of Science & Technology in Shenzhen, Shenzhen Virtual University Park, Shenzhen 518000, People's Republic of China

1. K. Maeda, K. Teramura, D. Lu, T. Takata, N. Saito, Y. Inoue and K. Domen, *Nature*, 2006, **440**, 295.
2. S. Moniz, S. A. Shevlin, D. Martin, Z. Guo and J. Tang, *Energ. Environ. Sci.*, 2015, **8**, 731.
3. A. Kudo and Y. Miseki, *Chem. Soc. Rev.*, 2009, **38**, 253.
4. L. Li, P. A. Salvador and G. S. Rohrer, *Nanoscale*, 2014, **6**, 24.
5. P. D. Tran, L. H. Wong, J. Barber and J. S. Loo, *Energ. Environ. Sci.*, 2012, **5**, 5902.
6. A. Fujishima and K. Honda, *Nature*, 1972, 37-38.
7. B. Liu and E. S. Aydil, *J. Am. Chem. Soc.*, 2009, **131**, 3985.
8. P. D. Cozzoli, A. Kornowski and H. Weller, *J. Am. Chem. Soc.*, 2003, **125**, 14539.
9. K. Hund-Rinke and M. Simon, *Environ. Sci. Pollut. R.*, 2006, **13**, 225.
10. I. Robel, M. Kuno and P. V. Kamat, *J. Am. Chem. Soc.*, 2007, **129**, 4136.
11. S. D. Burnside, V. Shklover, C. Barbé, P. Comte, F. Arendse, K. Brooks and M. Grätzel, *Chem. Mater.*, 1998, **10**, 2419.
12. K. Zhu, N. R. Neale, A. Miedaner and A. J. Frank, *Nano Lett.*, 2007, **7**, 69.
13. H. Imai, Y. Takei, K. Shimizu, M. Matsuda and H. Hirashima, *J. Mater. Chem.*, 1999, **9**, 2971.
14. C. A. Grimes, *J. Mater. Chem.*, 2007, **17**, 1451.
15. Z. Miao, D. Xu, J. Ouyang, G. Guo, X. Zhao and Y. Tang, *Nano Lett.*, 2002, **2**, 717.
16. J.-M. Wu, H. C. Shih and W.-T. Wu, *Nanotechnology*, 2006, **17**, 105.
17. J. M. Macak and P. Schmuki, *Electrochimica Acta*, 2006, **52**, 1258.
18. Z. Zhang, M. F. Hossain and T. Takahashi, *Int. J. Hydrogen Energ.*, 2010, **35**, 8528.
19. D. Wang and L. Liu, *Chem. Mater.*, 2010, **22**, 6656.
20. Z. Zhang, Y. Yuan, Y. Fang, L. Liang, H. Ding, G. Shi and L. Jin, *J. Electroanal. Chem.*, 2007, **610**, 179.
21. A. L. Linsebigler, G. Lu and J. T. Yates Jr, *Chem. Rev.*, 1995, **95**, 735.
22. E. Hendry, M. Koeberg, B. O'Regan and M. Bonn, *Nano lett.*, 2006, **6**, 755.
23. G. K. Mor, O. K. Varghese, M. Paulose, K. Shankar and C. A. Grimes, *Sol. Energ. Mater. Sol. C.*, 2006, **90**, 2011.
24. X.-F. Gao, H.-B. Li, W.-T. Sun, Q. Chen, F.-Q. Tang and L.-M. Peng, *J. Phys. Chem. C*, 2009, **113**, 7531.
25. M. Ni, M. K. Leung, D. Y. Leung and K. Sumathy, *Renew. Sust. Energ. Rev.*, 2007, **11**, 401.
26. P. Yu, K. Zhu, A. G. Norman, S. Ferrere, A. J. Frank and A. J. Nozik, *J. Phys. Chem. B*, 2006, **110**, 25451.
27. W. T. Sun, Y. Yu, H. Y. Pan, X. F. Gao, Q. Chen and L. M. Peng, *J. Am. Chem. Soc.*, 2008, **130**, 1124.
28. F.-X. Xiao, J. Miao, H.-Y. Wang and B. Liu, *J. Mater. Chem. A*, 2013, **1**, 12229-12238.
29. C. Ratanatawanate, A. Bui, K. Vu and K. J. Balkus Jr, *J. Phys. Chem. C*, 2011, **115**, 6175.
30. T.-L. Li, Y.-L. Lee and H. Teng, *J. Mater. Chem.*, 2011, **21**, 5089.
31. A. Kongkanand, K. Tvrdy, K. Takechi, M. Kuno and P. V. Kamat, *J. Am. Chem. Soc.*, 2008, **130**, 4007.
32. L. Yang, S. Luo, R. Liu, Q. Cai, Y. Xiao, S. Liu, F. Su and L. Wen, *J. Phys. Chem. C*, 2010, **114**, 4783.
33. J. Miao, H. B. Yang, S. Y. Khoo and B. Liu, *Nanoscale*, 2013, **5**, 11118-11124.
34. F.-X. Xiao, J. Miao, H.-Y. Wang, H. Yang, J. Chen and B. Liu, *Nanoscale*, 2014, **6**, 6727-6737.
35. S. Deka, A. Genovese, Y. Zhang, K. Miszta, G. Bertoni, R. Krahne, C. Giannini and L. Manna, *J. Am. Chem. Soc.*, 2010, **132**, 8912.

 This journal is © The Royal Society of Chemistry 2015

36. M. Dhanam, P. K. Manj and R. R. Prabhu, *J. Cryst. Growth*, 2005, **280**, 425.
37. J. Choi, N. Kang, H. Y. Yang, H. J. Kim and S. U. Son, *Chem. Mater.*, 2010, **22**, 3586.
38. S. C. Riha, D. C. Johnson and A. L. Prieto, *J. Am. Chem. Soc*, 2010, **133**, 1383.
39. Y. X. Hu, M. Afzaal, M. A. Malik and P. O'Brien, *J. Cryst. Growth*, 2006, **297**, 61.
40. Q. J. Guo, H. W. Hillhouse and R. Agrawal, *J. Am. Chem. Soc*, 2009, **131**, 11672.
41. G. Zoppi, I. Forbes, R. Miles, P. J. Dale, J. J. Scragg and L. M. Peter, *Prog. Photovolt.: Res. Appl.*, 2009, **17**, 315.
42. S. HyukáIm and J. HyeokáPark, *Chem. commun.*, 2010, **46**, 2385.
43. H. Kim, M. Seol, J. Lee and K. Yong, *J. Phys. Chem. C*, 2011, **115**, 25429.
44. H. Wang, W. Zhu, B. Chong and K. Qin, *Int. J. Hydrogen Energ.*, 2014, **39**, 90.
45. K. Machado, J. De Lima, T. Grandi, C. Campos, C. Maurmann, A. Gasperini, S. Souza and A. Pimenta, *Acta Crystallogr. Sect. B: Struct. Sci.*, 2004, **60**, 282.
46. W. Zhu, X. Liu, H. Liu, D. Tong, J. Yang and J. Peng, *J. Am. Chem. Soc*, 2010, **132**, 12619.
47. Y.-G. Kim, J. Y. Kim, D. Vairavapandian and J. L. Stickney, *J. Phys. Chem. B*, 2006, **110**, 17998.
48. R. Vaidyanathan, J. L. Stickney and U. Happek, *Electrochimica acta*, 2004, **49**, 1321.
49. M. K. Mathe, S. M. Cox, B. H. Flowers Jr, R. Vaidyanathan, L. Pham, N. Srisook, U. Happek and J. L. Stickney, *J. Cryst. Growth*, 2004, **271**, 55-64.
50. J. L. Stickney, *Adv. Electrochem. Sci. Eng.*, 2002, **7**, 1.
51. V. Venkatasamy, N. Jayaraju, S. Cox, C. Thambidurai, U. Happek and J. Stickney, *J. Appl. Electrochem.*, 2006, **36**, 1223.
52. F. Loglio, M. Innocenti, F. D'acapito, R. Felici, G. Pezzatini, E. Salvietti and M. Foresti, *J. Electroanal. Chem.*, 2005, **575**, 161.
53. I. Sisman, M. Alanyalioglu and Ü. Demir, *J. Phys. Chem. C*, 2007, **111**, 2670.
54. İ. Y. Erdoğan and Ü. Demir, *J. Electroanal. Chem.*, 2009, **633**, 253.
55. Y.-L. Lee, C.-F. Chi and S.-Y. Liau, *Chem. Mater.*, 2009, **22**, 922.
56. K.-H. Lin, C.-Y. Chuang, Y.-Y. Lee, F.-C. Li, Y.-M. Chang, I.-P. Liu, S.-C. Chou and Y.-L. Lee, *J. Phys. Chem. C*, 2011, **116**, 1550.
57. C.-F. Chi, H.-W. Cho, H. Teng, C.-Y. Chuang, Y.-M. Chang, Y.-J. Hsu and Y.-L. Lee, *Appl. Phys. Lett.*, 2011, **98**, 012101.
58. Y. L. Lee and Y. S. Lo, *Adv. Fun. Mater.*, 2009, **19**, 604.
59. ~~K. Shankar, J. I. Basham, N. K. Allam, O. K. Varghese, G. K. Mor, X. Feng, M. Paulose, J. A. Seabold, K.-S. Choi and C. A. Grimes, *J. Phys. Chem. C*, 2009, **113**, 6327-6359.~~

Electronic Supplementary Information

Highly Efficient Photoanode Based on Cascade Structural Semiconductor of $Cu_2Se/CdSe/TiO_2$: A Multifaceted Approach to Achieving Microstructural and Compositional Controls

Baohe Chong,[abc] Wen Zhu,*[abc] Yong Liu,[a] Li Guan[b] and George Z. Chen*[b]

[a] State Key Laboratory of Materials Processing and Die & Mould Technology, Huazhong University of Science & Technology, Wuhan 430074, People's Republic of China

[b] Department of Chemical and Environmental Engineering, The University of Nottingham, Nottingham NG7 2RD, United Kingdom

[c] Research Institute of Huazhong University of Science & Technology in Shenzhen, Shenzhen Virtual University Park, Shenzhen 518000, People's Republic of China

Email: wen.zhu@nottingham.ac.uk (W. Zhu), Geroge.Chen@nottingham.ac.uk (G.Z. Chen)

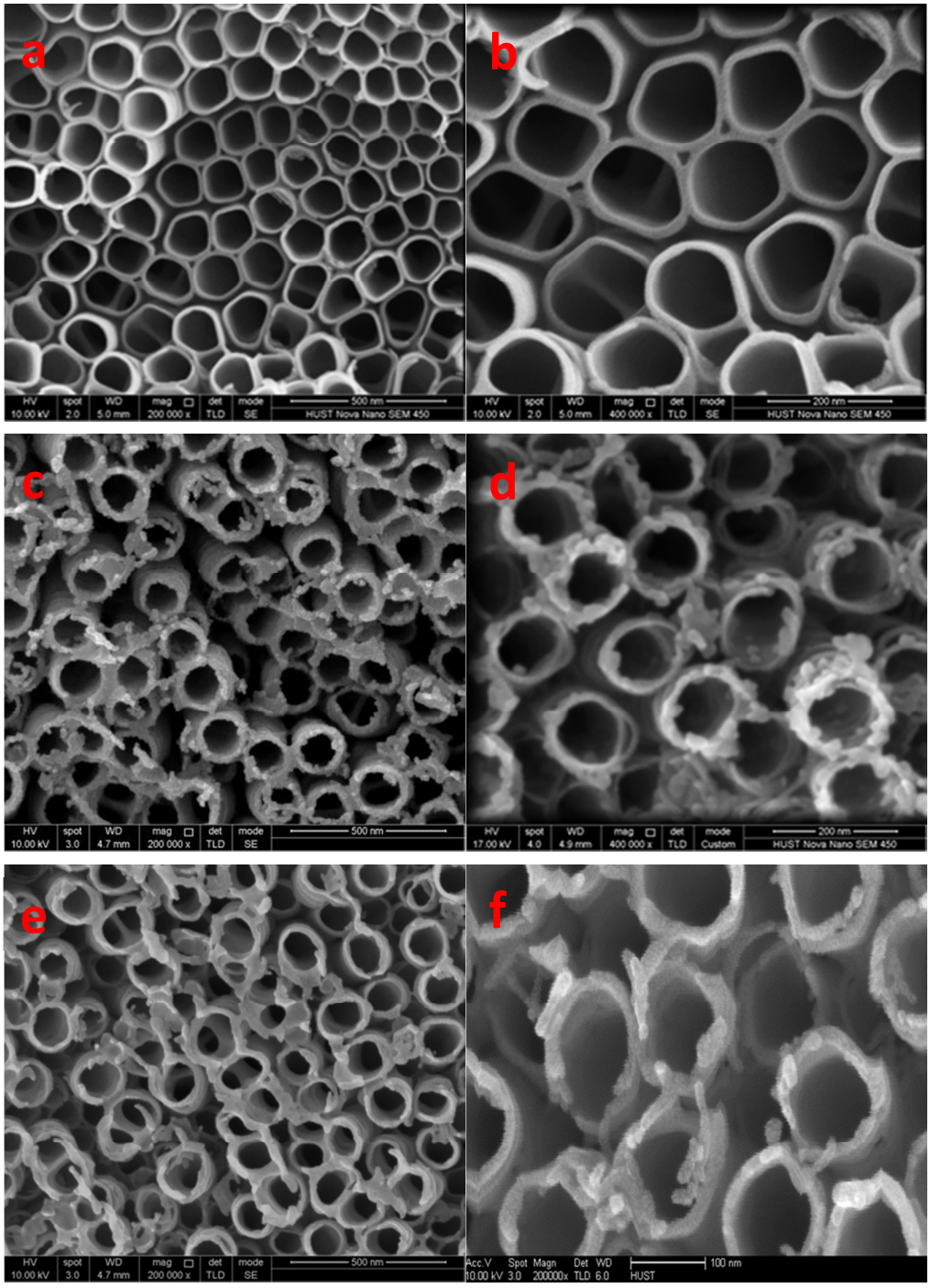

Figure S1. FESEM images of top-surface: (a,b) pure TiO_2, (c,d) CdSe(7h)/TiO_2, (e,f) CdSe(1h)/Cu(0.6C)/CdSe(6h)/TiO_2

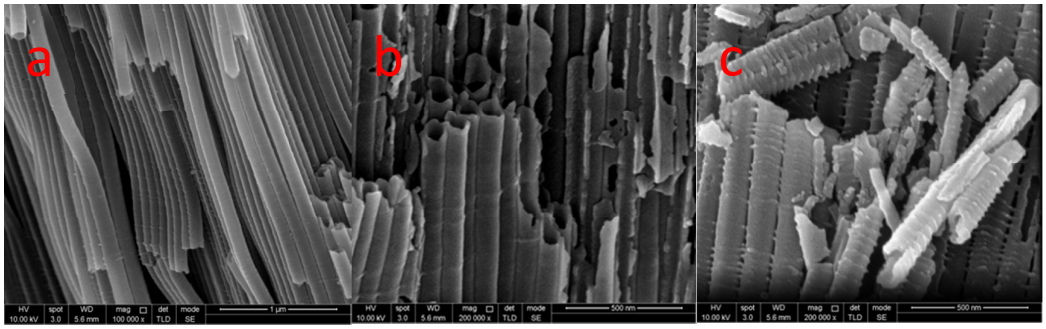

Figure S2. Cross-sectional FSEM images of pure TiO_2 (a), CdSe/TiO_2 (b) and CdSe(1h)/Cu(0.6C)/CdSe(6h)/TiO_2 (c).

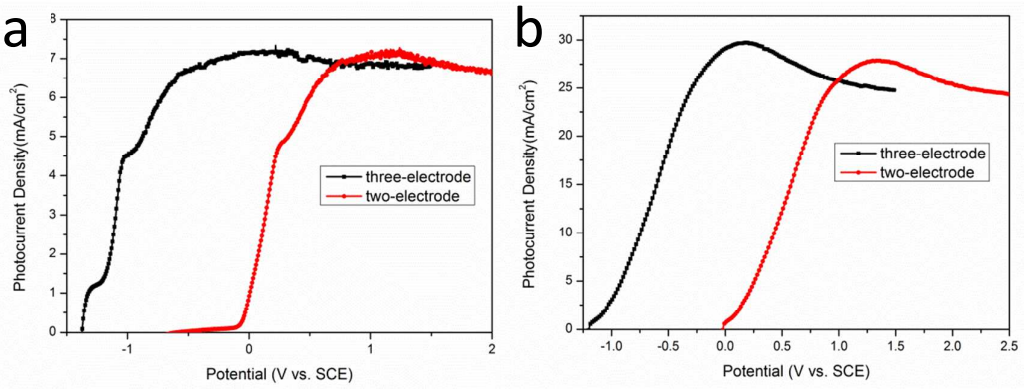

Figure S3. (a) Photocurrent density curves of CdSe/TiO_2 NTAs in different configuration, (b) Photocurrent density curves of Cu_2Se/CdSe/TiO_2 NTAs in different configuration.